**HEFAT2012**
**9th International Conference on Heat Transfer, Fluid Mechanics and Thermodynamics**
**16 – 18 July 2012**
**Malta**

# SPACER GRID EFFECTS ON THE HEAT TRANSFER ENHANCEMENT DURING A REFLOOD

Sang-Ki Moon*, Seok Cho, Byoung-Jae Kim, Jong-Kuk Park, Young-Jung Youn
*Author for correspondence
Thermal Hydraulics Safety Research Division,
Korea Atomic Energy Research Institute,
1045 Daedeok-daero, Yuseong-gu, Daejeon, 305-353
Republic of Korea
E-mail: skmoon@kaeri.re.kr

## ABSTRACT

An experimental study using 6x6 and 2x2 square lattice rod bundles has been performed to investigate the effects of spacer grids on the heat transfer enhancement during a bottom-reflood phase. The spacer grids improve a turbulent mixing of flow and induces breakup of large droplets into smaller ones. These result in the heat transfer enhancement between the fuel rods and the surrounding fluid. Since the geometry of the spacer grid affects the turbulent mixing and droplet breakup behaviors, three types of spacer grids with different geometry were tested in the present study. In order to investigate the heat transfer enhancement by spacer grids, single-phase steam cooling and droplet breakup by spacer grid were separately investigated.

For the convective heat transfer enhancement in single-phase steam flow, the heater rod surface temperatures were measured in the vicinity of the space grid. In single-phase steam cooling experiment, the heat transfer was enhanced at upstream and downstream of spacer grids. Downstream of the spacer, the heat transfer enhancement decays with the distance from the top end of the spacer grid exponentially. The heat transfer enhancement depends on the Reynolds number as well as the flow blockage ratio. A new empirical correlation was developed in order to account for the effect of the Reynolds number.

For the droplet breakup experiment, the sizes and velocities of droplets were measured across the spacer grid. The droplet breakup ratio decreases with increasing the Weber number of the droplet impacting on the spacer grid. The droplet breakup ratio by spacer grids was relatively higher than conventional correlations.

## INTRODUCTION

In a nuclear reactor, spacer grids support the fuel rods and maintain proper geometrical configuration of fuel rods within a rod bundle assembly. The spacer grids alternate the thermal-hydraulic behaviors near the spacer grids. They reduce the flow area by contracting the flow and then expanding it downstream of the spacer grid. Thus, the flow and thermal boundary layers are disrupted and re-established by the spacer grid. This enhances the local heat transfer within and downstream of the spacer grid. The droplet breakup behavior by spacer grid largely depends on the geometry of the spacer grid. When the spacer grid is not wetted by liquid film, large droplets impacting on the spacer grid are split into a large number of smaller ones, thereby increasing the surface area for droplet evaporation. On the other hand, in the wetted grid, droplets are entrained from the liquid films deposited on the grid surface. In this case, the downstream droplet size can be larger or smaller than the upstream droplet size. The sizes of the entrained droplets mainly depend on the wetting condition and geometry of the spacer grid.

## NOMENCLATURE

| | | |
|---|---|---|
| $A$ | [-] | Fitting constant |
| $b$ | [-] | Fitting constant |
| $D_h$ | [m] | Hydraulic diameter |
| $d_{32}$ | [m] | Sauter mean diameter of droplets |
| $d_o$ | [m] | Diameter of impacting droplets |
| $h$ | [W/m$^2$°C] | Heat transfer coefficient |
| $k_s$ | [W/m°C] | Thermal conductivity of steam |
| $Nu$ | [-] | Nusselt number |
| $q''$ | [W/m$^2$] | Heat flux |
| $Re$ | [-] | Reynolds number |
| $T_w$ | [°C] | Heater surface temperature |
| $T_s$ | [°C] | Steam temperature |
| $v_d$ | [m/s] | Droplet velocity |
| $We$ | [-] | Weber number of impacting droplets |
| $x$ | [m] | Axial distance from the top of spacer grid |
| $Z$ | [m] | Axial distance along the heated section |

Special characters

| | | |
|---|---|---|
| $\varepsilon$ | [-] | Blockage ratio |
| $\rho$ | [kg/m$^3$] | Density of droplets |
| $\sigma_d$ | [N/m] | Surface tension of droplets |

Subscripts

| | |
|---|---|
| 0 | Without heat transfer enhancement |
| down | Downstream of spacer grids |
| max | Maximum |
| s | Steam |
| up | Upstream of spacer grids |

For these reasons described above, various experimental and theoretical studies have been performed to examine the effects of spacer grids on the heat transfer enhancement during reflood phase. When single-phase steam flow occurs in the early phase of the reflood, the cladding temperature may increase abruptly and reaches usually a maximum value due to the low heat transfer from the fuel to the steam. Hence, it is of importance to elucidate the effect of the spacer grid on the heat transfer enhancement in single-phase steam flow. Yao et al. [1] reported that the heat transfer between wall and steam shows the maximum value at the top end of the spacer grid and that the Nusselt number decays exponentially downstream of the spacer grid. They developed an empirical correlation that only takes into account the flow blockage ratio and is applicable for simple egg-crate types of grids. An improved correlation was derived by Groeneveld et al. [2] to provide a correct asymptotic trend for both single-phase and two-phase flow. This correlation is based on the Yao et al.'s correlation. Holloway et al. [3, 4] carried out heat transfer enhancement experiments using standard grids and mixing vane grids.

The conventional correlations for the heat transfer enhancement by spacer grids in single-phase steam flow have an exponential decay function and do not take into account hydrodynamic (i.e, Reynolds number) effects. Recently, Miller et al. [5] showed that the decay function is affected by not only the blockage ratio but also the flow Reynolds number. They reported that the heat transfer enhancement decreases with the Reynolds number.

As for droplet breakup by spacer grids, a lot of attempts have been made to quantify and elucidate the droplet breakup by the spacer grid [6, 7, 8, 9]. The previous studies are useful to gain insight into the hydrodynamics and heat transfer phenomena of droplets breakup by spacer grid. However, they are based on the experiments using artificially generated droplets by injecting subcooled water though a nozzle ahead of a grid spacer. A few studies have been carried out using naturally generated droplets during the reflood. Sugimoto and Murao [10] conducted experiments in a 6×6 rod bundle and the Sauter mean diameter ratio between upstream and downstream of spacer grids was 0.89~0.97 for a dry grid. They developed an empirical correlation whose droplet breakup was dependent on the blockage ratio. Cheung and Bajorek [11] developed a semi-empirical correlation to predict the droplet breakup size downstream of the spacer grid. This correlation states that the droplet breakup size depends on the Weber number, the blockage ratio, and the kinetic energy of the impacting droplets required to convert to the surface energy of the newly-generated droplets. The Cheung and Bajorek's correlation is only applicable to dry spacer grids in droplet flow.

The present study deals with two kinds of heat transfer enhancement phenomena by spacer grids. First, the heat transfer enhancement by a spacer grid was investigated in single-phase steam flow. Several types of spacer grids were tested in order to investigate the effects of spacer grid geometries on the heat transfer enhancement in single-phase steam flow. The Reynolds number effect on the heat transfer enhancement was studied in order to clarify the hydrodynamic effects. Second, the droplet breakup behaviours were investigated with naturally generated droplets during a real reflood situation.

## EXPERIMENTAL FACILITIES AND METHOD

Spacer grid effects on the heat transfer enhancement during a reflood have been investigated using two kinds of rod bundle, i.e., 6x6 and 2x2 rod bundles. Figure 1 shows a schematic diagram of the 6x6 rod bundle reflood test facility, ATHER (Advanced Thermal Hydraulic Evaluation of Reflood phenomena), which consists of a test section, a separating system for measuring the amount of entrained liquid droplet, a pressure oscillation damping system to control the system pressure, a coolant supply system, and a steam supply system. A single-phase steam generated in the steam generator can be injected into the bottom of the test section. Figure 2 shows the cross-sectional view of the 6x6 rod bundle. The rod bundle consists of 30 heater rods, 2 unheated rods, and a guide tube in the center of the bundle, which have prototypic geometry of APR1400 (Korean nuclear power plants) reactor core. In the figure, G1, G2, and G3 stand for the rod group numbers which have different axial locations of thermocouples for the measurement of heater surface temperatures as shown in Fig. 3. The star symbol indicates the location at which the fluid temperature is measured. The heated length and diameter of the heater rods are 3.81 m and 9.5 mm, respectively. The heater rods with a pitch of 12.85 mm are located in a 6x6 square array and heated indirectly by AC (alternating current) power. The sheath and heating element of the heater rods are made of Inconel 600 and Nichrome, respectively. A total of 11 spacer grids were installed to support the heater rods along the axial location in the test section. The spacer girds have the same geometry with those used in Korean nuclear power plant, i.e., APR1400. For instrumented heater rods, six K-type thermocouples with a sheath diameter of 0.5 mm are embedded on the outer surface of the heater rod to measure the heater rod surface temperature. The total number of thermocouples for measuring the wall temperature of heater rods is 96. A total of 17 thermocouples are installed along the heated section to measure the fluid temperature. The temperatures of flow housing and guide tube are also measured using thermocouples. Figure 3 indicates the locations of the thermocouples, pressure taps, visualization windows, and the spacer grids. Figure 4 shows the axial power distribution along the heater rods. The heated section is divided into 15 steps to simulate a symmetric cosine axial heat flux profile. The radial power distribution is uniform, so that the heater rods have the same power.

From the measured data, the local Nusselt number can be calculated from the heat flux, wall and steam temperatures as follows:

$$Nu = hD_h / k_s = q'' D_h / [k_s (T_w - T_s)]. \quad (1)$$

The estimated uncertainties for the Nusselt number was ±3.2%.

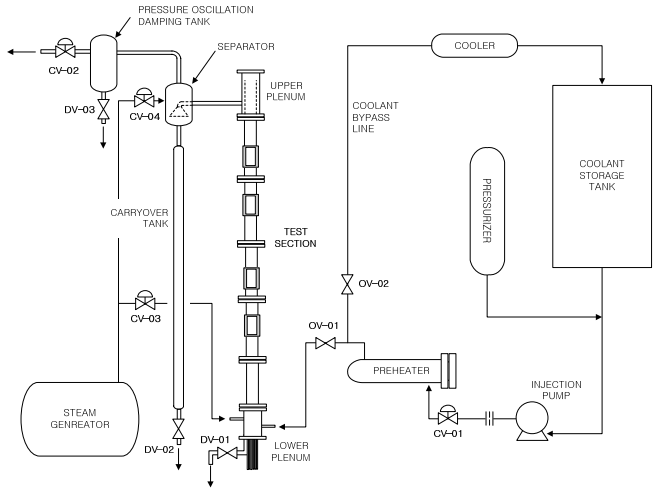


**Figure 1** Schematic diagram of ATHER facility

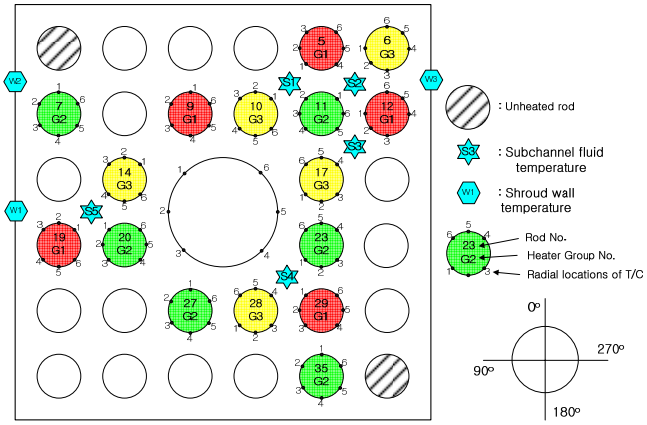


**Figure 2** Rod bundle configuration and radial locations of temperature measurement

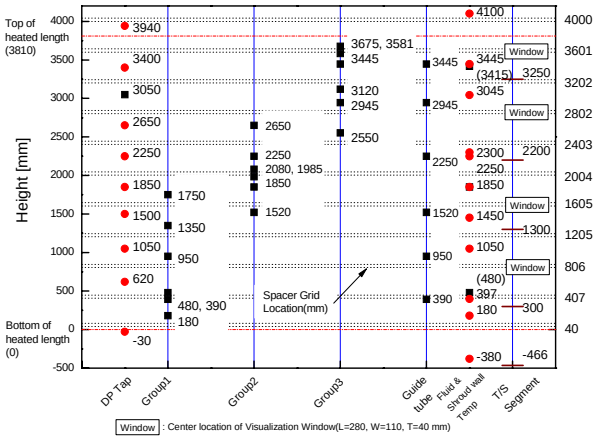


**Figure 3** Axial locations of temperature measurements

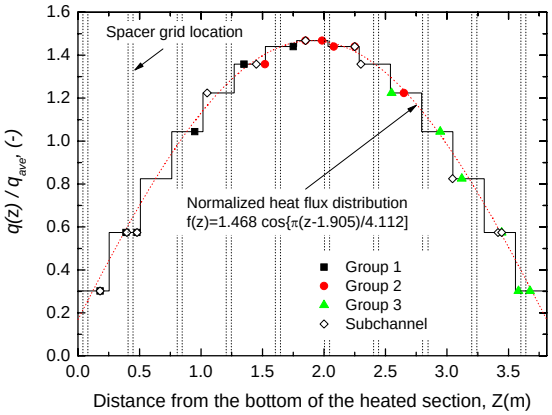


**Figure 4** Axial power shape of a 6x6 rod bundle

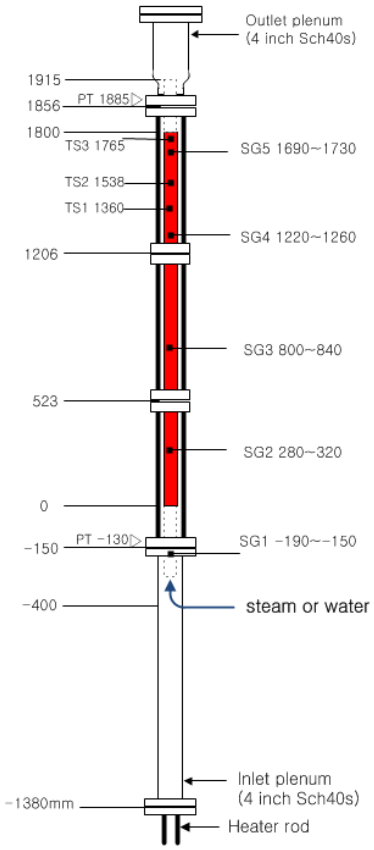


**Figure 5** Schematic diagram of 2x2 rod bundle test section

Figure 5 shows the schematic diagram of the test section used in 2x2 rod bundle experiment. The heater rods have the heated length of 1.8 m. The heater rods have an outer diameter of 20 mm and pitch of 27 mm, respectively. A total of five spacer grids are installed to support heater rods. SG1 ~ SG5 indicate the axial locations where spacer grids are installed. A uniform electrical power in both the axial and radial directions is supplied to the heater rods. Figure 6 shows the rod bundle geometry and typical simple spacer grid used in the 2x2 rod bundle. Three types of spacer grids are used in the 2x2 rod

bundle experiment as shown in Table 1. The major differences of spacer grids are the flow blockage ratio and the mixing vane angle. Type 1 spacer grid does not have the mixing vanes as a reference case. Types 2 and 3 are designed to investigate the effect of the blockage ratio.

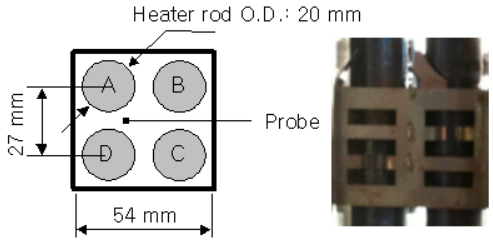


**Figure 6** Heater rods and spacer grid

**Table 1** Spacer grid used in 2x2 rod bundle

| Type | Vane | Vane angle | blockage ratio |
|---|---|---|---|
| Type 1 | No | - | 0.17 |
| Type 2 | Yes | 60° | 0.35 |
| Type 3 | Yes | 67° | 0.41 |

## HEAT TRANSFER ENHANCEMENT IN SINGLE PHASE STEAM FLOW

Single-phase steam flow experiments were performed in the 2x2 and 6x6 rod bundles. Figure 7 shows the typical wall temperature along the axial distance for the steam flow rate of 0.0149 kg/s ($Re$ = 9283 at spacer grid SG 2 and $Re$ = 8235 at the spacer grid SG 3 in Fig. 5) in the 2x2 rod bundle. In the graph, $Z$ is the axial distance from the bottom of the heated section. As shown in the figure, the wall temperature is greatly reduced near the spacer grids, and after that the wall temperature increases with axial distance from the spacer grids. This means that the heat transfer coefficients are significantly increased near the spacer grids and then decreased with downstream of the spacer grids. The steam temperatures were measured at the axial locations of 1360 and 1535 mm. The steam temperature increases linearly with the axial distance, and thus the local steam temperature along the heat section is obtained by extrapolation of the measured ones.

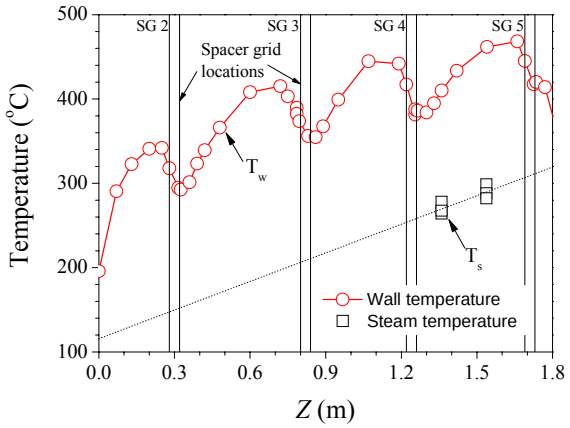


**Figure 7** Wall temperature profile along the heated length

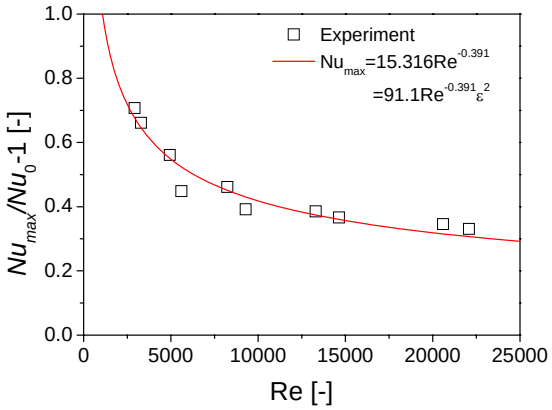


**Figure 8** Maximum Nusselt number against Reynolds number

Figure 8 plots the maximum Nusselt number ($Nu_{max}$) against Reynolds number ($Re$) for the spacer grid SG 2 and SG 3 in the 2x2 bundle. The applied power is 8 kW. The outlet of test section is exposed to the atmosphere. The pressure in the test section is approximately 0.13 MPa. In general, the Nusselt numbers have maximum values at the exit of the spacer grid and then decreases with increasing distance downstream of the spacer grid. The value of $Nu_{max}/Nu_0$-1 is a measure how much the convective heat transfer increases by spacer grids. $Nu_0$ is the Nusselt number when spacer grids are assumed to be absent. $Nu_0$ is of vital importance in dimensionless analysis on heat transfer enhancement. In general, $Nu_0$ is computed by using an empirical correlation. However, the existing correlations yield different values of $Nu_0$ with the experimentally measured ones at quite downstream of spacer grids where the effects of spacer grids on the heat transfer seems to be disappeared. In addition, an accurate prediction is quite difficult due to a lack of empirical correlations applicable for the present rod bundle geometry. As a consequence, $Nu_0$ was experimentally set by the Nusselt number just ahead of the spacer grid where the wall temperature shows a local maximum value ($x$ = 200 mm for SG 2 and $x$ = 600 mm for SG 3). It is observed in Fig. 8 that the maximum Nusselt number decreases with increasing Reynolds number. A new correlation can be derived by fitting experimental data as follows:

$$\frac{Nu_{max}}{Nu_0} - 1 = 15.316 Re^{-0.391} = 91.1 Re^{-0.391} \varepsilon^2 \qquad (2)$$

In the derivation, it is assumed that $Nu_{max}/Nu_0$-1 is proportional to the square of the blockage ratio as the previous studies did [1-5]. Previous studies stated that $Nu_{max}/Nu_0$-1 is only a function of the blockage ratio. Recently, Miller et al. (2011) reported that $Nu_{max}/Nu_0$-1 depends on the Reynolds number as well as the blockage ratio. The present data also shows the similar behavior. In Fig. 8, the heat transfer enhancement does not change much when the Reynolds number is so high that the flow is turbulent. This is because that turbulent flow structure does not change much if the Reynolds number is greater than a certain value. However, at the low Reynolds numbers, the flow structure is easy to change by spacer grids; the mixing vane plays a significant role in agitating steam flow compared with

weak turbulent mixing at low Reynolds numbers so that the convective heat transfer can be more enhanced. Thus, the heat transfer enhancement is higher in low Reynolds numbers than in high Reynolds numbers. Equation 2 will be applied to the Type 2 spacer grid for a validation.

Most previous studies adopted an exponential decay function to predict the heat transfer enhancement downstream of the spacer grid. Accordingly, the heat transfer enhancement starts to decay right downstream of the spacer grid. However, the present experimental data shows that a Gaussian function is more appropriate for the prediction of the heat transfer enhancement as follows:

$$\frac{Nu(x)}{Nu_0} - 1 = A \exp\left( -b \left( \frac{x}{D_h} \right)^2 \right) \qquad (3)$$

Here, $Nu(x)$ is the local Nusselt number at the distance $x$ from the trailing edge of the spacer grid main body, not from the mixing vane tip. The variable $D_h$ is the hydraulic diameter. The parameters $A$ and $b$ should be determined from experimental data. $A$ and $b$ are assumed to be a function of the Reynolds number as well as the blockage ratio. The parameter $A$ is equal to $Nu_{max}/Nu_0$-1 in Fig. 8.

Figures 9 ~ 13 show the experimental data for the 2x2 rod bundle. In the figures, the main body of the spacer grid is located between $x/D_h$ = -2.7~0. As shown in the figures, the experimental data can be fitted with Eq. (3) over the wide range of the Reynolds number. Our main focus is the downstream region of the spacer grid. It can be found that $A = Nu_{max}/Nu_0$-1 decreases with increasing the Reynolds number. The variable $b$ in the fitting curves is plotted in Fig. 14 as a function of the Reynolds number. One can see that $b$ is relatively constant when the Reynolds number is sufficiently high, i.e., in turbulent flow. The reason is that the turbulent mixing is strong enough to suppress the heat transfer enhancement by spacer grids. When fitting the experimental data, the determination of the constant $b$ might be subjective. Hence, we tried to use the same $b$ for all experimental data as possible. As shown in Figs. 9 ~ 13, the constant $b$ predicts well the experiment data in the turbulent flow. The Yao et al.'s correlation [1] is plotted together for a comparison. The Yao et al.'s correlation does not take into account the effect of the Reynolds number.

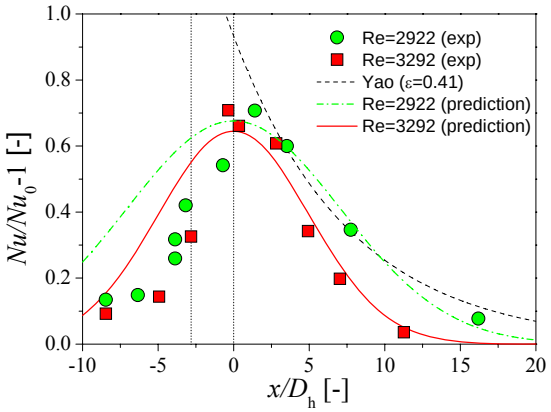


**Figure 9** *Nu* (*Re* = 2922, 3292) in 2x2 rod bundle test

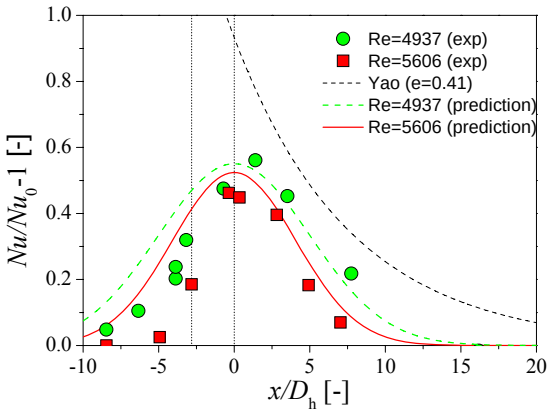


**Figure 10** *Nu* (*Re* = 4937, 5606) in 2x2 rod bundle test

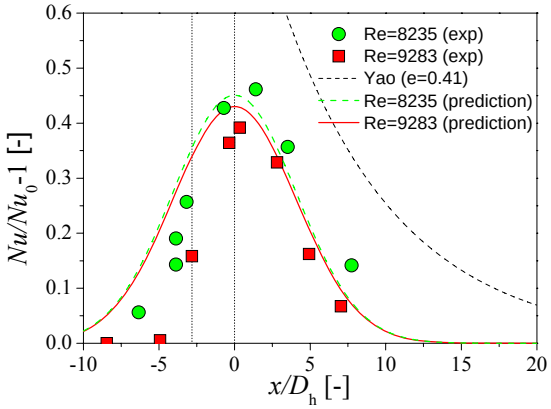


**Figure 11** *Nu* (*Re* = 8235, 9283) in 2x2 rod bundle test

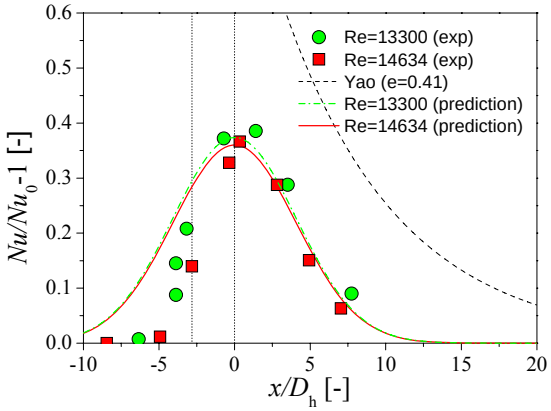


**Figure 12** *Nu* (*Re* = 13300, 14634) in 2x2 rod bundle test

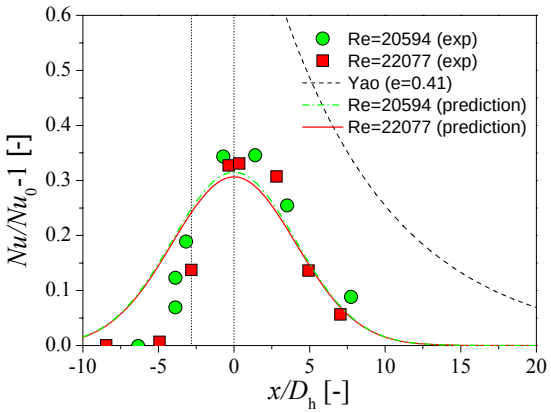


**Figure 13** *Nu* (*Re* = 20594, 22077) in 2x2 rod bundle test

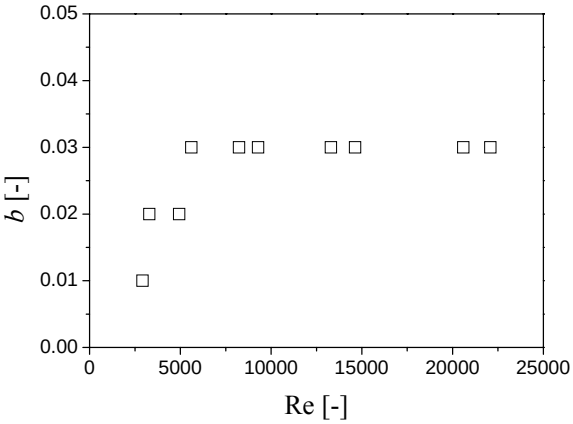


**Figure 14** Decay value with Reynolds number

A similar equation form to Eq. 3 was applied to the 6x6 rod bundle experiment. The 6x6 rod bundle experiments were performed with two different heater powers. Four different steam flow rates were used for each heater power. Unlike the 2x2 test facility, the temperature measurement points are axially sparse because of the long heated length and a lot of heater rods. Figure 15 shows the analysis results for the spacer grid located at 2050 mm from the bottom of heated section. One can see that the applied heater power does not affect the experimental result. However, the steam flow rates influence on the heat transfer enhancement. The steam flow rates 50 g/s and 80 g/s correspond to the Reynolds numbers of 6500 and 10750, respectively. The value of $A$ (= $Nu/Nu_0$-1) decreases with increasing the Reynolds number. This behavior is also observed in the 2x2 rod bundle test. Due to the limitation of the axial data points, $A$ is fitted with a linear function of the Reynolds number as follows:

$$\frac{Nu_{max}}{Nu_0} - 1 = (-2.882 \times 10^{-4} Re + 8)\varepsilon^2 \qquad (4)$$

The values of $b$ are not much different for two fitting curves. Due to the different rod bundle geometry, $A$ and $b$ may be different. However, general trends are the similar in both rod bundles.

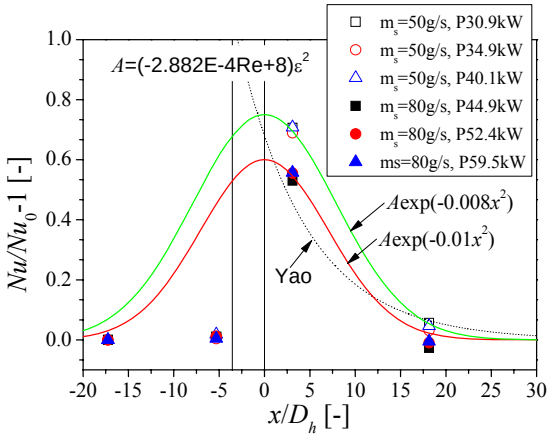


**Figure 15** *Nu* (*Re* = 6500, 10750) in 6x6 rod bundle test

## DROPLET BEHAVIOR IN REFLOOD CONDITIONS

The droplet breakup behaviors were observed in the 2x2 rod bundle facility under nearly atmosphere pressure. When the wall temperature attained to a steady-state value, subcooled water (nearly 40 °C) was injected though the bottom of the test section. The power was adjusted as such that the maximum wall temperature was maintained to about 500 °C (in Case 1, 0.4 kW/rod) or 700 °C (in Case 2, 0.5 kW/rod) at the steady-state. The reflood velocity was 1 cm/s.

A Xenon lamp was used to illuminate droplets. Droplet images were recorded by a high-speed camera (Redlake MotionXtra HG-100K). Image pairs were made of two successive images with the time interval 0.2 ms. The time interval between image pairs was 20 ms. A VisiSize software (Oxford Lasers Ltd.) was used to extract the velocities and sizes of droplets by means of image processing.

Single-phase steam flow occurs in the early stage of the reflood. Droplets start to appear at about 10 seconds after the reflood initiation. Clear droplet image continues up to about 30 s and 40 s for the Case 1 and Case 2, respectively. Beyond the times, the measurement window becomes so wetted that image processing cannot be applied. Tables 2 and 3 show the statistical analysis results on the droplet breakup behavior. Since the experiment was transient, the analysis was performed for every 10 seconds. It was found that the period of 10 seconds contains hundreds of droplets, which is enough for the statistical analysis. As shown in Tables 3 and 4, the droplet diameter increases as the reflood time passes.

**Table 2** Droplet analysis (Case 1)

| time [s] | upstream | | downstream | |
|---|---|---|---|---|
| | $d_{32}$[μm] | $v_d$[m/s] | $d_{32}$[μm] | $v_d$[m/s] |
| 0~10 | - | - | - | - |
| 10~20 | 510 | 4.5 | 456 | 3.9 |
| 20~30 | 748 | 4.5 | 556 | 4.2 |
| 30~40 | 1173 | 6.8 | 856 | 5.0 |

**Table 3** Droplet analysis (Case 2)

| time [s] | upstream | | downstream | |
|---|---|---|---|---|
| | $d_{32}$[μm] | $v_d$[m/s] | $d_{32}$[μm] | $v_d$[m/s] |
| 0~10 | - | - | - | - |
| 10~20 | 466 | 5.4 | 456 | 4.2 |
| 20~30 | 1031 | 4.9 | 930 | 4.3 |

Figure 16 plots the droplet breakup size. Sugimoto and Murao [10] reported that the droplet breakup ratio was 0.89 ~ 0.97 for a dry grid. As shown in the figure, the breakup ratios are similar to the values measured by Sugimoto and Murao. The breakup ratio is relatively high in the limited range of $We_d$ in the real reflood, compared with experimental data for artificially generated droplets. Smaller droplets have higher interfacial area. In this case, heat transfers for wall-to-droplets and wall-to-fluid can be enhanced by the increased interfacial area. Therefore, the droplet breakup ratio is an important parameter. According to the previous studies, the breakup ratio decreases with increasing Weber number because the droplet speed impacting on spacer grids increases with increasing Weber number. However, the previous studies also revealed that the breakup ratio is more than 0.8 and relatively constant for low Weber numbers. From these findings, one can say that during the reflood, the Weber number is relatively low so that the droplet breakup ratio is relatively high.

Meanwhile, Cheng and Bajorek [11] proposed a correlation for predicting the droplet diameter in a dry spacer grid, based real reflood experiments. Their correlation does not include any information on the steam.

$$\frac{d_{32}}{d_0} = \left(1 + 0.1803\varepsilon \mathrm{We}_0^{0.558}\right)^{-1} \quad (5)$$

Here, $d_{32}$ and $d_0$ denote the Sauter mean diameter of the outgoing droplets and the diameter of the impacting droplet on the spacer grids. Equation 5 uses the assumption that the impacting droplets have a uniform size distribution, and it is applicable to a dry spacer grid in dispersed droplet flow. In the present study, $d_0$ is replaced by the Sauter mean diameter of the impacting droplets, as Cheng and Bajorek did. The symbol $\varepsilon$ represents the fraction of impacting droplets undergoing breakup, which is not the exactly same as the blockage ratio, but closely related to the blockage ratio. The droplet Weber number impacting on the spacer grid is defined as $We_0 = \rho_d v_d^2 d_0 / \sigma_d$. The correlation of Cheung and Bajorek is plotted in Fig. 16 for a comparison. The value of $\varepsilon$ = 0.05 agrees with the present data, which is much less than the blockage ratio 0.41 of the present spacer grid. This difference can be explained by two reasons. One is the exclusive applicability of the correlation to a dry grid. In the early stage of the reflood, the spacer grid is dry, but the spacer grid gets wetted with increasing the time. The other is that $\varepsilon$ in the Cheung and Bajorek correlation is not the same as the blockage ratio.

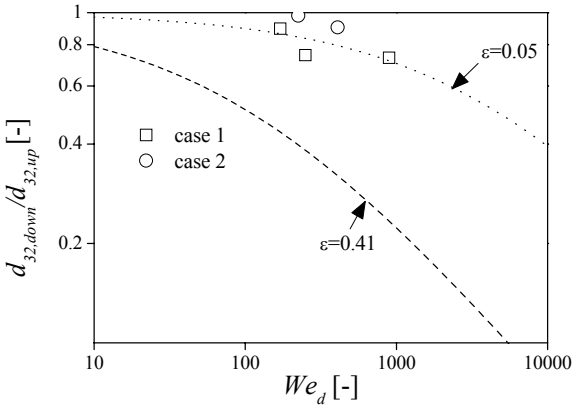


**Figure 16** Droplet breakup size

## CONCLUSIONS

Experiments have been done to investigate the effects of spacer grids on the heat transfer enhancement during reflood in a nuclear reactor. As a result, a new single-phase heat transfer enhancement correlation was developed to predict the heat transfer enhancement downstream of the spacer grid in single-phase steam flow. The single-phase heat transfer enhancement was a function of the Reynolds number as well as the flow blockage ratio. The heat transfer enhancement was higher in low Reynolds numbers than in high Reynolds numbers. The heat transfer enhancement was relatively constant when the Reynolds number is so high that the flow is turbulent. The reason is that turbulent flow structure does not change much by spacer grids if the Reynolds number is greater than a certain value. However, given the low Reynolds numbers, the flow structure is easy to change by spacer grids; the mixing vane play a relatively significant role in agitating steam flow so that the convective heat transfer is enhanced at low Reynolds numbers. The Nusselt number was shown to exponentially decay with a Gaussian function as going downstream of spacer grid.

In the meanwhile, another experiment was made to measure the droplet breakup ratio across the spacer grid during the real reflood. It was found that the breakup ratio is relatively high during reflood, compared with experimental results using artificial injection of droplets. The breakup ratio decreases with increasing Weber number because the droplet speed impacting on spacer grids increases with increasing Weber number. During the reflood, the Weber number is low so that the droplet breakup ratio is relatively high. The conventional correlation for the droplet breakup ratio does not show a good prediction for the present experimental data.

## ACKNOWLEDGMENT

This work was supported by the Nuclear Research & Development of the Korea Institute of Energy Technology

Evaluation and Planning (KETEP) grant funded by the Korea Government Ministry of Knowledge Economy.

## REFERENCES

[1] Yao, S. C., Hochreiter, L. E., and Leech, W. J., Heat-Transfer Augmentation in Rod Bundles Near Grid Spacers, *Transactions of the ASME*, Vol. 104, pp.76-81, 1982.

[2] Groeneveld, D.C., et al., A General Method of Predicting Critical Heat Flux in Advanced Water-Cooled Reactors, *9th International Topical Meeting on Nuclear Reactor Thermal Hydraulics (NURETH-9)*, San Francisco, USA, October 3-8, 1999.

[3] Holloway, M. V., McClusky, H. L., Beasley, D. E., and Conner, M. E., The Effect of Support Grid Features on Local, Single-Phase Heat Transfer Measurements Rod Bundles, *J. of Heat Transfer*, Vol. 126, pp.43-53, 2004.

[4] Holloway, M. V., Beasley, D. E., and Conner, M. E., Single-Phase Convective Heat Transfer in Rod Bundles, *Nuclear Eng. and Design*, Vol. 238, pp.848-858, 2008.

[5] Miller, D., Cheung, F. B., and Bajorek, S. M., On the Development of a Grid-Enhanced Single-Phase Convective Heat Transfer Correlation, *14th International Topical Meeting on Nuclear Reactor Thermal-hydraulics (NURETH-14)*, Toronto, Canada, September 25-30, 2011.

[6] Adams, J. E. and Clare, A. J., Droplet Breakup and Entrainment at PWR Spacer Grids, *NUREG/CP-0060*, 590-614, USNRC, Washington, 1984.

[7] Lee, L., Cho, S. K., and Sheen, H. J., A Study of Droplet Hydrodynamics Across a Grid Spacer, *NUREG/CR-4034*, USNRC, Washington, 1984a.

[8] Lee, S. L., Sheen, H. J., Cho, S. K., and Issapour, I. Measurement of Droplet Dynamics Across Grid Spacer in Mist Cooling of Subchannel of PWR, *NUREG/CP0060*, pp.619-642, USNRC, Washington, 1984b.

[9] Cho, H. K, Choi, K. Y., Cho, S., Song, C. H., Experimental Observation of the Droplet Size Change Across a Wet Grid Spacer, *Nuclear Eng. and Design*, Vol.241, pp.4649-4656, 2011.

[10] Sugimoto, J. and Murao, Y., Effect of Grid Spacers on Reflood Heat Transfer in PWR-LOCA, *J. of Nuclear Science and Technology*, Vol. 21, p.103-114, 1984.

[11] Cheung, F. B. and Bajorek, S. M., Dynamics of droplet breakup through a grid spacer in a rod bundle, *Nuclear Engineering and Design*, Vol. 241, pp.236-244, 2010.